

Applicability Assessment of a Thermo-Formed Piezoelectret Accelerometer in Agricultural Robotics Systems

Igor Nazareno Soares*, Ruy Alberto Corrêa Altafim*, Ruy Alberto Pisani Altafim†

*Department of Electrical and Computer Engineering, Engineering School of São Carlos
University of São Paulo
São Carlos, Brazil

†Department of Computer Systems, Informatics Center
Federal University of Paraíba
João Pessoa, Brazil

e-mail: igor.soares@usp.br, altafim@usp.br, ruy@ci.ufpb.br

Abstract—The advancement of robotic systems in precision agriculture has increased the demand for robust, cost-effective, and customizable inertial sensors capable of operating in diverse mechanical environments. This work evaluates the applicability of a custom-developed Thermo-Formed Piezoelectret Accelerometer (TFPA) for use in agricultural robotics. The sensor, composed of a thermo-formed piezoelectret, a 30 g seismic mass, and a polyurethane foam support, was experimentally characterized over a frequency range of 50 Hz to 3.2 kHz. The sensor was calibrated using a back-to-back method with a reference accelerometer. The measured sensitivity reached a peak of 196 mV/g at 100 Hz, exhibiting a frequency response typical of a second-order underdamped system. An analytical mass–spring–damper model was developed to simulate the sensor’s transfer function, and parameter tuning demonstrated strong agreement with experimental results. By comparing the TFPA’s response with vibration frequency bands reported in the literature for Unmanned Aerial Vehicles (UAV), gear-driven implements, robotic arms, and harvesters, the sensor was found to be suitable for mid-to high-frequency applications, and capable of operating at even higher frequencies with signal amplification. Design parameters, such as foam thickness and Young’s modulus, were shown to enable application-specific tuning of resonance and sensitivity. The TFPA’s performance, mechanical robustness, and tunability highlight the potential of piezoelectret-based accelerometers for embedded vibration sensing in agricultural automation. Future work will focus on miniaturization, electronics integration, and extended calibration toward lower frequencies.

Keywords—Piezoelectret accelerometers; vibration sensing; agricultural robotics; inertial sensors; dynamic modeling; resonance tuning; sensor calibration; frequency response analysis.

I. INTRODUCTION

The integration of robotic technologies in agriculture has significantly advanced the efficiency, precision, and sustainability of farming operations. Applications ranging from autonomous tractors and robotic arms for harvesting to Unmanned Aerial Vehicles (UAV) for monitoring and spraying have become increasingly prevalent in both research and commercial deployments [1]–[3]. These robotic systems often operate in complex, dynamic environments, subject to terrain-induced vibrations, actuator-induced oscillations, and mechanical impacts that can degrade both system performance and sensor accuracy.

Monitoring and analyzing vibration in agricultural machinery is essential for tasks, such as structural health monitoring,

fault detection in powertrains, optimization of robotic motion control, and enhancement of operator safety and comfort [4]–[6]. Accelerometers are a core component in these sensing applications, typically required to operate over a wide frequency range and withstand harsh environmental conditions.

Conventional accelerometers — such as Micro-Electro-Mechanical Systems (MEMS) and piezoelectric types — are widely used but may face limitations in specific agricultural robotic applications. MEMS devices, for instance, tend to have reduced accuracy at higher frequencies or under large mechanical stress, while commercial piezoelectric sensors may be costly or require complex conditioning electronics [7].

In this context, piezoelectret-based accelerometers have emerged as a promising alternative due to their mechanical robustness, low cost, lightweight construction, and potential for customization [8]–[10]. Piezoelectrets are polymeric materials with quasi-permanent internal polarization that generate charge in response to mechanical deformation. A class of advanced materials that have garnered significant attention in scientific research and technological innovation, akin to piezoelectric polymers, they exhibit piezoelectric properties, yet are distinguished by their cellular microstructure and enhanced performance characteristics [11]. The remarkable electromechanical coupling efficiency and flexibility inherent in piezoelectrets render them particularly appealing for developing compact, lightweight, and versatile transducers and actuators [12]. When integrated with a seismic mass and elastic suspension, they can serve as effective vibration transducers [8]–[10].

This work builds upon previous research involving the development of a Thermo-Formed Piezoelectret Accelerometer (TFPA), shifting the focus toward evaluating its applicability in agricultural robotics. The sensor — composed of a thermo-formed piezoelectret element with an integrated lead seismic mass and compliant foam support — was previously characterized in terms of design and frequency response [9][10]. In this study, the TFPA is further examined through experimental calibration and analytical mass–spring–damper modeling, with emphasis on mapping its sensitivity profile to the vibration environments typical of robotic systems, such as UAVs, automated harvesters, rotary cultivators, and robotic

arms. The objective is to determine the sensor's suitability for these applications by identifying the overlap between its linear response range and the dominant operational frequencies observed in the field, while also exploring mechanical tuning strategies and signal amplification techniques to broaden its functional range for practical deployment.

The remainder of this paper is organized as follows. Section II reviews related work on vibration profiles in agricultural robotics and sensor requirements. Section III details the design, construction, and calibration of the proposed TFPA sensor. Section IV presents the experimental results, theoretical modeling, and application-specific analysis. Finally, Section V concludes the study and outlines directions for future work.

II. LITERATURE REVIEW

Vibration analysis is a key consideration in the design, operation, and maintenance of robotic systems in agriculture. Each class of agricultural machine or robotic component presents characteristic vibration profiles, often dictated by actuation mechanisms, mechanical loads, and environmental interactions. Understanding these profiles is essential for selecting or designing compatible sensors, such as accelerometers.

A. Vibration Sources in Agricultural Robotics

Rotary Implements and Powertrains. Rotary tillers, cultivators, and gear-driven implements generate moderate to high-frequency vibrations due to blade impacts, gear meshing, and chassis resonance. Gao et al. [13] conducted a comprehensive analysis of the vibration characteristics of a tractor-rotary cultivator combination, identifying multiple frequency domains of significance. In the low-frequency range (0–100 Hz), strong energy was observed around 33 Hz in the tractor, attributed to its first-order natural frequency, and operator-sensitive cab vibrations were noted between 4.9 Hz and 6.8 Hz. In the medium-frequency range (100–500 Hz), resonance frequencies appeared around 280 Hz for the tractor cab and 350 Hz for the rotary tiller gearbox. Additionally, the rotary tiller showed less energy at low frequencies but exhibited increasing vibration activity above 250 Hz, consistent with efficient soil interaction. The gearbox demonstrated substantial high-frequency content between 750 and 1000 Hz, underscoring the mechanical complexity and resonance behavior in operational conditions.

UAVs and Aerial Systems. Drones used for crop monitoring and spraying are subject to vibrational loads arising from rotor dynamics, motor RPM fluctuations, and rapid maneuvers. Power Spectral Density (PSD) analysis has shown that UAVs exhibit distinct vibration bands depending on operational conditions. Vibrations in the 10–70 Hz range are typically linked to shaft and blade rotation at moderate throttle levels, while more intense vibrational energy occurs between 70 and 230 Hz due to high-speed rotor excitations during fast maneuvers. These frequency domains are particularly important for sensor stability and data quality in precision agriculture applications [14].

Harvesters and Cutting Mechanisms. Combine harvesters and robotic harvesters experience complex, multi-modal vibrations. Meng et al. [15] analyzed the modal response of sugar beet combine harvesters and identified significant vibration modes at 12.7 Hz due to the power input shaft and around 35 Hz related to engine excitation. In robotic harvesting systems, vibratory tools are often tuned to specific frequencies to optimize fruit detachment efficiency. Zheng et al. [16] reported optimal frequency ranges between 10 and 20 Hz for winter jujube trees, using harmonic response and transient analysis based on high-resolution 3D reconstruction. Similarly, Sola-Guirado et al. [17] assessed vibration parameters for lateral canopy shakers used in olive harvesting, highlighting the need for precise frequency targeting to maximize fruit removal while minimizing energy input.

Robotic Arms and Manipulators. Robotic arms used in fruit picking or soil sampling are subject to structure-borne resonance and actuation-induced oscillations. Badkoobehzadeh et al. [3] conducted finite element and experimental modal analysis on a 5-Degrees-Of-Freedom (5-DOF) long-reach robotic arm designed for agricultural applications. Their study identified natural frequencies ranging from 4.4 Hz to 41.6 Hz, depending on the arm's configuration and payload, with lower modes associated with structural bending and torsional responses.

Sprayers and Operator Cabins. In large boom sprayers, low-frequency oscillations can arise from terrain coupling and the flexible dynamics of long boom arms, often requiring vibration damping systems to ensure uniform spraying. Qiu et al. [18] analyzed a spray boom-air suspension system designed to mitigate these vibrations but did not specify particular frequency ranges. Regarding operator cabins, Cutini et al. [19] reported that Whole-Body Vibration (WBV) in agricultural tractors typically occurs in the frequency range of 0.5 Hz to 80 Hz, which can pose health risks to operators if sustained for prolonged periods. These findings underscore the importance of vibration management in agricultural vehicle design.

B. Sensor Compatibility Considerations

The wide spectrum of vibration frequencies in agricultural robotics — ranging from sub-Hertz to several hundred Hertz — poses a challenge for accelerometer design. Sensors must not only detect vibrations across this range but also maintain signal linearity and adequate sensitivity. Commercial MEMS accelerometers may offer sufficient resolution at low frequencies, but often lack robustness and bandwidth for higher-frequency diagnostics. Piezoelectric sensors offer excellent high-frequency response but are typically more costly and less suited to large-scale deployment or customization [7].

The TFPA aims to fill this niche by offering a scalable, mechanically tunable alternative with sensitivity and bandwidth characteristics that can be matched to specific robotic applications.

III. MATERIALS AND METHODS

This section describes the experimental and analytical procedures used to evaluate the TFPA. It is divided into three subsections: the first details the design and physical construction of the sensor; the second presents the calibration method used to determine its frequency response; and the third outlines the analytical modeling approach based on a mass–spring–damper system to simulate the sensor’s behavior under dynamic excitation.

A. Design and Construction of the TFPA

The developed TFPA, shown in Figure 1a, is based on a custom-fabricated piezoelectret film formed by thermal lamination of fluorinated ethylene propylene (FEP) layers, as can be seen in Figure 1c. The lamination process creates four open tubular voids, which become polarized and acquire electromechanical sensitivity after a high-voltage corona charging process. The internal microstructure behaves as a ferroelectret, producing an electric signal in response to mechanical deformation perpendicular to the film plane [20].

The piezoelectret film is coated with vacuum-deposited aluminum electrodes and coupled mechanically to a seismic mass of 30 g, composed of lead and shaped as a 10 mm-high cylinder with 18 mm diameter. This mass is housed inside a low-friction polytetrafluoroethylene (PTFE) sheath that ensures mechanical alignment and isolates lateral forces. An elastic element made of polyurethane foam, with density of 12 kg/m³, provides vertical restoring force and allows free oscillation of the mass along the sensing axis, as can be seen in Figure 1b. This configuration constitutes a single-axis, inertia-based accelerometer.

The sensing structure is enclosed within an aluminum casing measuring 74 mm in height and 51 mm in diameter. A coaxial Bayonet Neill-Concelman (BNC) connector is integrated for electrical output, with shielding ensured by the metallic housing. The final assembly offers mechanical robustness, electrical shielding, and modularity suitable for embedded applications in robotic platforms.

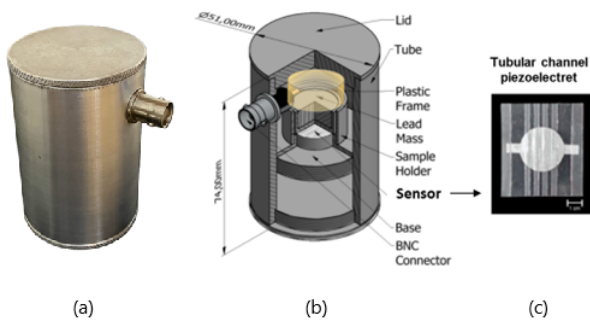


Figure 1. (a) Constructed TFPA prototype (b) TFPA internal structure (c) Piezoelectret sensor with open tubular channels

B. Calibration Procedure

The TFPA’s frequency response, spanning from 50 Hz to 3.2 kHz, was characterized using the experimental setup

illustrated in Figure 2 [10]. A function generator (HP model 33120A) was used to produce sinusoidal excitation signals, which were fed into a Brüel & Kjær (B&K) model 2707 power amplifier. This amplifier drove a B&K 4812 electrodynamic shaker to induce controlled vertical vibrations.

The TFPA and a reference piezoelectric accelerometer (B&K model 8305) were co-mounted atop the shaker platform to ensure identical excitation. The reference signal passed through a B&K Type 2635 conditioning amplifier, while the TFPA output was recorded directly, without additional amplification. Both signals were captured simultaneously by an Agilent Technologies DSO-X 3024A digital oscilloscope, allowing synchronized time-domain acquisition and accurate amplitude comparisons.

The system was calibrated to generate a constant sinusoidal acceleration amplitude of 9.81 m/s² (1 g). Sensitivity in mV/g was computed for each frequency point. This experimental data were used to identify resonance behavior, verify model predictions, and determine the operational frequency range where the sensor exhibits linear sensitivity.

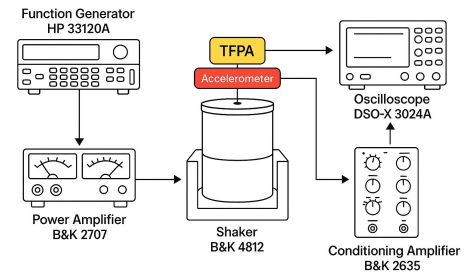


Figure 2. Experimental calibration setup showing signal generator, amplifier, shaker, TFPA and reference accelerometer

C. Analytical Modeling and Simulation

To interpret and predict the sensor behavior under dynamic excitation, the TFPA was modeled as a Single-Degree-Of-Freedom (SDOF) mass–spring–damper system [21]. The governing differential equation is:

$$m\ddot{x}(t) + c\dot{x}(t) + kx(t) = F(t) \quad (1)$$

Here, m is the seismic mass, k is the effective stiffness of the foam, and c represents the damping coefficient. Under sinusoidal base excitation, the response was simulated in the frequency domain by evaluating the transfer function between the base acceleration and the acceleration of the seismic mass.

The elastic modulus of the foam (E) was estimated from manufacturer datasheets and literature for low-density polyurethane foams, typically ranging from 50–200 kPa [22]. The stiffness was calculated as $k = EA/L$, where A is the contact area between the foam and the mass, and L is the foam thickness.

Parametric studies were performed by varying m , E , and L to assess tuning capabilities and validate the match between experimental and theoretical frequency responses.

IV. RESULTS AND DISCUSSIONS

This section presents and analyzes the results obtained from the TFPA's experimental characterization and theoretical modeling. The first subsection discusses the measured frequency response of the sensor and its resonant behavior. The second compares these experimental results with theoretical simulations. The third examines the sensor's compatibility with typical vibration profiles in agricultural robotics, and the final subsection addresses limitations of the current prototype and opportunities for future miniaturization.

A. Experimental Frequency Response

The TFPA's measured frequency response, shown in Figure 3 [10], displays a clear resonant peak centered at 100 Hz, where the sensor achieves a maximum sensitivity of approximately 196 mV/g. The sensitivity rises sharply toward this peak and falls off symmetrically beyond it, exhibiting the characteristic bell-shaped behavior of a second-order underdamped system.

Notably, the sensor does not present a flat linear region before resonance; instead, the sensitivity increases markedly between 50 Hz and 100 Hz. This non-flat rise suggests the influence of the resonance even slightly below the peak frequency. Beyond 100 Hz, the sensitivity decreases steeply and monotonically, with values dropping below 10 mV/g by 3.2 kHz. This confirms a narrow high-sensitivity band centered around the resonance and a progressively diminishing response at higher frequencies.

The experimental data confirms that the sensor operates as a classic mass–spring–damper resonant system and provides a well-defined dynamic signature suitable for matching with analytical models and mapping to real-world vibration profiles in agricultural robotics.

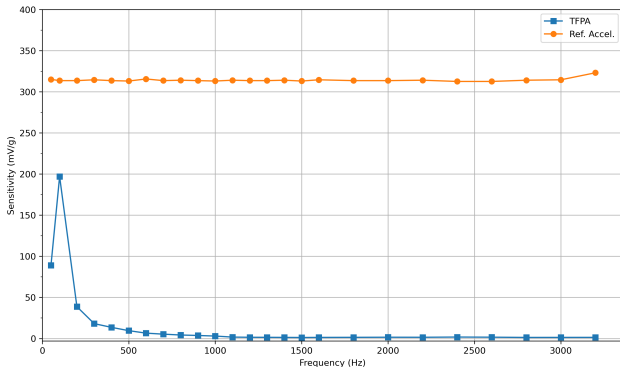


Figure 3. Frequency response of the TFPA, with a resonance frequency at 100 Hz

B. Comparison with Theoretical Models

To assess the fidelity of the TFPA's dynamic behavior, the experimentally obtained frequency response was compared to simulated models derived from a single-degree-of-freedom (SDOF) mass–spring–damper system. The transfer function used represents the mechanical gain between base excitation

and seismic mass acceleration, following the classical SDOF vibration theory for underdamped systems [21][23]. These challenges are common in mechanical systems and have been extensively addressed in vibration engineering practice [24].

$$H(j\omega) = \left| \frac{X''(j\omega)}{Y''(j\omega)} \right| = \frac{1}{\sqrt{(1-(\omega/\omega_n)^2)^2 + (2\zeta\omega/\omega_n)^2}} \quad (2)$$

where $\omega_n = \sqrt{k/m}$ is the undamped natural frequency, ζ is the damping ratio, and $k = EA/L$ is the effective stiffness of the foam element, with E representing Young's modulus, A the contact area, and L the foam thickness.

To illustrate the effect of key physical parameters on the sensor's dynamic behavior, preliminary simulations were conducted using three distinct configurations (A, B, and C), varying the seismic mass m , foam modulus E , and thickness L . These configurations produced resonance frequencies from approximately 30 Hz to 178 Hz, demonstrating the tunability of the system, as can be seen in Figure 4. Although none of these aligned precisely with the experimental response, they highlight the potential for application-specific optimization through mechanical design.

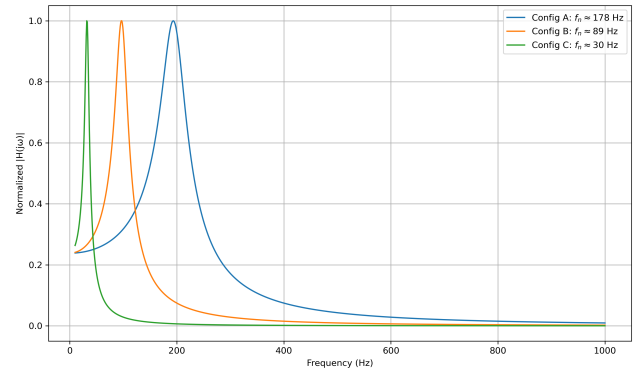


Figure 4. Simulated frequency responses for configurations A, B, and C, illustrating resonance tunability via changes in mass, stiffness, and foam thickness

A matched simulation was then performed using the known mass (30 g) and foam thickness ($L = 20$ mm). To align the model with the experimentally observed resonance, the required foam modulus was calculated and a damping ratio selected to reproduce the experimentally observed peak width and roll-off gradient.

Figure 5 shows the comparison between the experimental and simulated sensitivity curves. The matched model accurately reproduces the resonance peak and the roll-off profile beyond 100 Hz. This agreement validates the modeling approach and confirms the TFPA's characterization as a second-order inertial sensor. The mechanical parameters used in the simulation directly reflect physical sensor properties, demonstrating the model's predictive power for application-oriented tuning.

This result validates the mass–spring–damper model and confirms the TFPA's behavior as a second-order inertial trans-

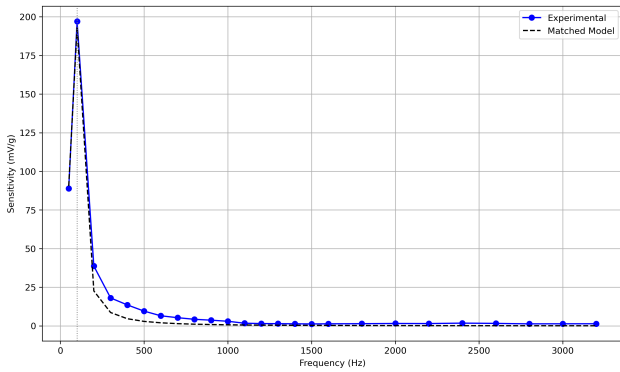


Figure 5. TFPA response comparison: experimental sensitivity data and matched simulation in physical units

ducer, whose performance can be predicted and tuned for agricultural applications.

C. Application Compatibility and Tuning Discussion

The validated dynamic model and measured frequency response of the TFPA enable a direct evaluation of its applicability across key classes of agricultural robotic systems, with respect to their dominant vibration frequency bands.

Based on the literature survey presented in Section II, the following typical operating frequencies were identified:

- **UAVs and electric motors (70–230Hz):** The TFPA's resonance at 100 Hz and its high sensitivity within the -3 dB bandwidth from 76 to 114 Hz make it well-suited for vibration monitoring in UAV propulsion systems and electric actuators, especially where higher-frequency diagnostics are required. Although the response drops off above resonance, it remains smooth and predictable, allowing for signal reconstruction with amplification techniques.
- **Gearboxes and rotary tillers (250–1000 Hz):** Although these frequencies lie above the TFPA's resonance, the sensor still provides measurable output in this range. Despite the lower gain, its linearity allows for reliable vibration detection, particularly when paired with signal conditioning or amplification techniques.
- **Robotic arms (4–40 Hz):** These structures operate below the TFPA's natural resonance. However, by modifying mechanical parameters — such as increasing the seismic mass or employing a more compliant foam — the resonance can be shifted downward, improving sensitivity in this domain.
- **Harvesting tools and vibratory shakers (10–35 Hz):** These tools often rely on carefully tuned excitation frequencies for fruit detachment. With proper tuning, the TFPA could be adapted for monitoring or feedback in such systems.
- **Sprayers and operator cabins (0.5–80 Hz):** While this range is outside the current operating band, a redesign with softer materials or mechanical amplification could enable compatibility. Additionally, whole-body vibration

monitoring may benefit from a broader-band solution incorporating the TFPA in multi-sensor systems.

These observations highlight the mechanical flexibility of the TFPA architecture. Because its resonance and bandwidth are governed by design-adjustable parameters — specifically the seismic mass m and the foam stiffness $k = EA/L$ — the sensor can be customized to target specific vibrational environments. Increasing stiffness or reducing mass shifts the response toward higher frequencies, while the opposite configuration favors low-frequency applications.

Overall, the current configuration positions the TFPA as a strong candidate for medium-frequency diagnostics, with a -3 dB bandwidth of 76–114 Hz, where the sensor exhibits high sensitivity and linearity. This aligns well with the dominant frequencies encountered in UAV propulsion systems and electric drivetrain components. Beyond this range, the sensor maintains a smooth and monotonic roll-off, with a measurable response verified experimentally up to 3.2 kHz, supporting its use in higher-frequency applications, such as gearboxes and rotary tillers.

While the sensor's sensitivity peaks near its 100 Hz resonance, the measured data confirm that its post-resonance behavior remains linear and predictable. This makes the TFPA viable for both resonance-tuned use cases and broadband diagnostic tasks — especially when paired with analog amplification, impedance matching, or digital signal processing. These characteristics reinforce the TFPA's potential as a compact, tunable, and cost-effective solution for vibration monitoring in embedded agricultural robotic systems.

D. Limitations and Opportunities for Miniaturization

While the TFPA demonstrates favorable sensitivity and mechanical tunability, its current prototype form factor — measuring 74 mm in height with a 30 g seismic mass — may constrain its deployment in compact robotic platforms. The use of a relatively large lead mass and thick polyurethane foam is primarily dictated by the target resonance frequency and mechanical alignment constraints in this version.

However, piezoelectret materials themselves are inherently thin, lightweight, and flexible, offering significant potential for miniaturization. Reducing the mass and housing dimensions would naturally raise the resonant frequency, allowing adaptation to higher-frequency vibration environments. To offset the resulting loss in sensitivity, amplification strategies — either through analog front-end electronics or high-impedance buffer stages — can be introduced without compromising signal fidelity.

Additionally, engineered elastomer materials with customized stiffness and damping characteristics could enable finer control over the sensor's dynamic range and resonance tuning. This modularity supports the development of application-specific TFPA variants optimized for distinct vibration profiles across agricultural robotic systems.

Overall, future design iterations should aim to balance mass reduction, material optimization, and electronic conditioning

to extend the TFPA's usability to both embedded and distributed sensing architectures in precision agriculture.

Importantly, the strong agreement between experimental data and the SDOF-based matched model further supports this pathway. It demonstrates the feasibility of predictive tuning in future designs, enabling model-driven optimization of foam stiffness, damping, and mass configurations for compact versions tailored to specific vibrational environments.

V. CONCLUSION AND FUTURE WORK

This work presented the design, calibration, and dynamic modeling of a TFPA aimed at agricultural robotic applications. The sensor, composed of a thermo-formed FEP piezoelectret, a 30 g seismic mass, and a polyurethane foam support, was experimentally characterized across a wide frequency range (50 Hz to 3.2 kHz) using sinusoidal base excitation.

The measured sensitivity peaked at approximately 196 mV/g near 100 Hz, exhibiting a frequency response consistent with an underdamped second-order system. A single-degree-of-freedom mass-spring-damper model was developed, and the simulated response showed excellent agreement with the experimental data when foam stiffness and damping were tuned to match the observed dynamics.

Comparison with vibration frequency bands reported in the literature confirmed that the TFPA is well-suited for mid-frequency components, with a -3 dB sensitivity range between 76 and 114 Hz, including UAVs and electric actuators, while remaining functional at higher frequencies up to 3.2 kHz. Although sensitivity decreases beyond resonance, the sensor maintains linear and predictable behavior, making it viable for broadband diagnostics when supported by amplification or signal conditioning.

The TFPA's response characteristics can be tailored through geometric and material parameters, such as seismic mass, foam thickness, and Young's modulus. This enables application-specific tuning of the resonance and bandwidth. While the current prototype size may limit its use in compact platforms, the thin and lightweight nature of piezoelectret films supports future miniaturization.

These results position the TFPA as a robust, low-cost, and mechanically tunable solution for embedded vibration sensing in precision agriculture, with strong potential for future integration into adaptive and distributed robotic systems.

Building upon these findings, subsequent efforts will address the miniaturization of the TFPA, facilitating its integration into compact robotic platforms. Experimental validation in real agricultural environments is planned to evaluate long-term performance and environmental resilience. Further work will extend the calibration procedure below 50 Hz to enhance low-frequency application capabilities.

ACKNOWLEDGMENT

The authors thank the Brazilian funding agencies CAPES and CNPq, the University of São Paulo (Electrical and Computer Department at Engineering School of São Carlos), the Federal University of Paraíba, and the Institute of Technological Research of São Paulo (Energy Infrastructure Laboratory).

REFERENCES

- [1] R. P. Sishodia, R. L. Ray, and S. K. Singh, "Applications of remote sensing in precision agriculture: A review," *Remote Sensing 2020, Vol. 12, Page 3136*, vol. 12, p. 3136, 2020.
- [2] T. Duckett, S. Pearson, S. Blackmore, and B. Grieve, "Agricultural robotics: The future of robotic agriculture," *UK-RAS White Papers*, 2018.
- [3] H. Badkoobehhezaveh, R. Fotouhi, Q. Zhang, and D. Bitner, "Vibration analysis of a 5-dof long-reach robotic arm," *Vibration 2022, Vol. 5, Pages 585-602*, vol. 5, pp. 585-602, 2022.
- [4] M. Hosseinpour-Zarnaq, M. Omid, and E. Biabani-Aghdam, "Fault diagnosis of tractor auxiliary gearbox using vibration analysis and random forest classifier," *Information Processing in Agriculture*, vol. 9, pp. 60-67, 2022.
- [5] J. Xu, T. Jing, M. Fang, P. Li, and Z. Tang, "Failure state identification and fault diagnosis method of vibrating screen bolt under multiple excitation of combine harvester," *Agriculture 2025, Vol. 15, Page 455*, vol. 15, p. 455, 2025.
- [6] J. H. Kim, J. T. Dennerlein, and P. W. Johnson, "The effect of a multi-axis suspension on whole body vibration exposures and physical stress in the neck and low back in agricultural tractor applications," *Applied Ergonomics*, vol. 68, pp. 80-89, 2018.
- [7] T. Wu *et al.*, "Research status and development trend of piezoelectric accelerometer," *Crystals 2023, Vol. 13, Page 1363*, vol. 13, p. 1363, 2023.
- [8] J. F. Alves *et al.*, "An accelerometer based on thermoformed piezoelectrets with open-tubular channels," *Annual Report - Conference on Electrical Insulation and Dielectric Phenomena, CEIDP*, vol. 2020-October, pp. 524-526, 2020.
- [9] I. N. Soares *et al.*, "New design for a thermo-formed piezoelectret-based accelerometer," in *ALLSENSORS 2023, The Eighth International Conference on Advances in Sensors, Actuators, Metering and Sensing*, IARIA, 2023, pp. 21-24.
- [10] I. N. Soares, R. A. C. Altafim, R. A. P. Altafim, and M. M. Tokoro, "Investigation of thermo-formed piezoelectret accelerometer under different electrodynamic vibration conditions," in *ALLSENSORS 2024, The Ninth International Conference on Advances in Sensors, Actuators, Metering and Sensing*, IARIA, 2024, pp. 32-37.
- [11] M. M. Moreira *et al.*, "Piezoelectrets: A brief introduction," *IEEE Sensors Journal*, vol. 21, pp. 22 317-22 328, 2021.
- [12] X. Qiu *et al.*, "Ferroelectrets: Recent developments," *IET Nanodielectrics*, vol. 5, pp. 113-124, 2022.
- [13] Y. Gao *et al.*, "Analysis of vibration characteristics of tractor-rotary cultivator combination based on time domain and frequency domain," *Agriculture 2024, Vol. 14, Page 1139*, vol. 14, p. 1139, 2024.
- [14] C. Ge, K. Dunno, M. A. Singh, L. Yuan, and L. X. Lu, "Development of a drone's vibration, shock, and atmospheric profiles," *Applied Sciences 2021, Vol. 11, Page 5176*, vol. 11, p. 5176, 2021.
- [15] J. Meng, Z. Li, W. Xian, F. Li, and Y. Li, "Modal response and vibration characteristics of sugar beet combine harvester frame," *Engenharia Agrícola*, vol. 44, e20240054, 2024.
- [16] Z. Zheng *et al.*, "Characterising vibration patterns of winter jujube trees to optimise automated fruit harvesting," *Biosystems Engineering*, vol. 248, pp. 255-268, 2024.
- [17] R. R. Sola-Guirado *et al.*, "Vibration parameters assessment to develop a continuous lateral canopy shaker for mechanical harvesting of traditional olive trees," *Spanish Journal of Agricultural Research*, vol. 14, e0204-e0204, 2016.
- [18] W. Qiu *et al.*, "Analysis of factors influencing vibration suppression of spray boom-air suspension for medium and small-scale high-clearance sprayers," *Sensors 2021, Vol. 21, Page 6753*, vol. 21, p. 6753, 2021.

- [19] M. Cutini, M. Brambilla, and C. Bisaglia, "Whole-body vibration in farming: Background document for creating a simplified procedure to determine agricultural tractor vibration comfort," *Agriculture 2017, Vol. 7, Page 84*, vol. 7, p. 84, 2017.
- [20] R. A. P. Altafim *et al.*, "Template-based fluoroethylenepropylene piezoelectrets with tubular channels for transducer applications," *Journal of Applied Physics*, vol. 106, p. 014 106, 2009.
- [21] D. J. Inman, *Engineering Vibration*, 4th ed. Pearson Education, 2013.
- [22] D. Zenkert, *An Introduction to Sandwich Construction*. EMAS Publishing, 1995.
- [23] S. S. Rao, *Mechanical Vibrations*, 6th ed. Pearson, 2017.
- [24] C. M. Harris and A. G. Piersol, *Harris' Shock and Vibration Handbook*, 5th ed. McGraw-Hill, 2002.